Efficient Sensitivity Analysis of Lossy Multiconductor Transmission Lines with Nonlinear Terminations

Anestis Dounavis, Ramachandra Achar and Michel Nakhla
Department of Electronics, Carleton University, Ottawa, Ontario, K1S 5B6
Tel (613) 520-5780; Fax: (613) 520-5708; Email: msn@doe.carleton.ca

***Abstract* -- An efficient approach for sensitivity analysis of lossy multiconductor transmission lines in the presence of nonlinear terminations, is described. Sensitivity information is based on the recently developed closed-form matrix-rational approximation based transmission-line model. The method enables sensitivity analysis of interconnect structures with respect to both electrical and physical parameters. An important advantage of the proposed approach is that the derivatives of the MNA matrices with respect to per-unit-length parameters are obtained analytically.**

I. Introduction

The ever increasing quest for higher-operating speeds, miniature devices and denser layouts has made the signal integrity analysis a challenging task. As signal frequencies are approaching the GHz range, the interconnect effects such as delay, crosstalk, ringing and distortion become the dominant factors limiting the overall performance of microelectronic/microwave systems. At higher frequencies, the length of the interconnect becomes a significant fraction of the operating wavelength, and conventional lumped impedance models become inadequate in describing the interconnect performance and transmission line models become necessary [1]-[7].

Recently, an efficient multiconductor transmission line (MTL) model based on closed-form matrix-rational approximation has become available [3]-[5]. It can also handle lossy as well as frequency-dependent parameters. Application of this new MTL model to the sensitivity analysis for optimization of high-speed interconnects in the presence of nonlinear terminations is presented in this paper.

II. Circuit Equations with Closed-Form MTL Model

Distributed networks in the presence of nonlinear elements can be expressed as

$$\begin{aligned} \boldsymbol{C}_\phi \dot{\boldsymbol{x}}_\phi(t) + \boldsymbol{G}_\phi \boldsymbol{x}_\phi(t) + \sum_{k=1}^{N_t} \boldsymbol{D_k} \boldsymbol{i_k}(t) + \boldsymbol{f}_\phi(\boldsymbol{x}_\phi(t)) &= \boldsymbol{b}_\phi(t) \\ \boldsymbol{I_k} &= \boldsymbol{Y_k}(s)\boldsymbol{V_k} \end{aligned} \quad (1)$$

where

- $\boldsymbol{x}_\phi(t)$ is a vector, which include node voltages appended by independent and dependent voltage source currents, inductor currents, nonlinear capacitor charge and nonlinear inductor flux waveform. $\boldsymbol{G}_\phi$, $\boldsymbol{C}_\phi$ are constant matrices describing the lumped memoryless and memory elements of the network, respectively. $\boldsymbol{b}_\phi(t)$ is a vector with entries determined by the independent voltage and current sources. $\boldsymbol{f}_\phi(\boldsymbol{x}_\phi(t))$ is a vector describing the nonlinear elements.
- $\boldsymbol{D_k} = [d_{i,j} \in \{0, 1\}]$, is a selector matrix that maps $\boldsymbol{i_k}(t)$, the vector of terminal currents entering the interconnect subnetwork *k*, into the node space of the network, where $i \in \{1, \ldots, n\}$, $j \in \{1, \ldots, 2m_k\}$ and m_k is the number of coupled signal conductors in subnetwork *k*. N_t is the number of distributed structures. $\boldsymbol{Y_k}(s)$ is the admittance parameters of interconnect *k* in the Laplace domain. $\boldsymbol{I_k}$ and $\boldsymbol{V_k}$ represent the Laplace terminal voltages and currents of interconnect *k*.

The distributed elements in (1) do not have a direct representation in the time-domain, leading to mixed frequency/time simulation difficulty. In order to overcome this problem, a closed-form MTL model based on matrix-rational approximation has been recently proposed [3]-[5]. This interconnect model is shown to be efficient, passive and suitable for passive model reduction techniques based on congruent transformations [5]-[6]. Using this interconnect macromodel, (1) can be expressed as

$$\boldsymbol{C}\frac{d}{dt}\boldsymbol{x}(t) + \boldsymbol{G}\boldsymbol{x}(t) + \boldsymbol{f}(\boldsymbol{x}(t)) = \boldsymbol{b}(t) \quad (2)$$

where

$$\boldsymbol{C} = \boldsymbol{G_a} + \sum_{k=1}^{N_t} \sum_i (\boldsymbol{\psi_i^k})^{\mathbf{T}} \boldsymbol{G_i^k} \boldsymbol{\psi_i^k}$$

$$\boldsymbol{G} = \boldsymbol{C_a} + \sum_{k=1}^{N_t} \sum_i (\boldsymbol{\psi_i^k})^{\mathbf{T}} \boldsymbol{C_i^k} \boldsymbol{\psi_i^k} \quad (3)$$

Here the matrices $\boldsymbol{G_a}$, $\boldsymbol{C_a}$, $\boldsymbol{f}(\boldsymbol{x}(t))$ and $\boldsymbol{b}(t)$ are obtained from $\boldsymbol{G}_\phi$, $\boldsymbol{C}_\phi$, $\boldsymbol{f}_\phi(\boldsymbol{x}_\phi(t))$ and $\boldsymbol{b}_\phi(t)$ by appending them by rows (and/or) columns that contain zeros to account for the extra state variables required for the stamp of the transmission line. Thus, $\boldsymbol{G_a}$, $\boldsymbol{C_a}$ and $\boldsymbol{b}(t)$ can be expressed in the following block form

$$G_a = \begin{bmatrix} G_\phi & 0 \\ 0 & 0 \end{bmatrix} \qquad C_a = \begin{bmatrix} C_\phi & 0 \\ 0 & 0 \end{bmatrix}$$

$$f(x(t)) = \begin{bmatrix} f_\phi(x_\phi(t)) \\ 0 \end{bmatrix} \qquad b(t) = \begin{bmatrix} b_\phi(t) \\ 0 \end{bmatrix} \tag{4}$$

The indices i, k represent the i^{th} subsection of the k^{th} interconnect. The subsections of each interconnect are obtained from the poles and zeros of the Padé rational model of the exponential function. In the case of real pole-zero subsections, they can be expressed as

$$G_i^k = \begin{bmatrix} \frac{d_k}{2a_{0,k}}G_k & 0 & \frac{d_k}{2a_{0,k}}G_k & U \\ 0 & \frac{a_{0,k}}{2d_k}R_k^{-1} & \frac{-a_{0,k}}{2d_k}R_k^{-1} & -U \\ \frac{d_k}{2a_{0,k}}G_k & \frac{-a_{0,k}}{2d_k}R_k^{-1} & \left(\frac{a_{0,k}}{2d_k}R_k^{-1} + \frac{d_k}{2a_{0,k}}G_k\right) & 0 \\ U & -U & 0 & 0 \end{bmatrix}$$

$$C_i^k = \begin{bmatrix} \frac{d_k}{2a_{0,k}}C_k & 0 & \frac{d_k}{2a_{0,k}}C_k & 0 \\ 0 & 0 & 0 & 0 \\ \frac{d_k}{2a_{0,k}}C_k & 0 & \frac{d_k}{2a_{0,k}}C_k & 0 \\ 0 & 0 & 0 & \frac{2d_k}{a_{0,k}}L_k \end{bmatrix} \tag{5}$$

Similar expression can be derived for the case of complex pole-zero subsection [4]-[5].

The matrices ψ_{ik}^{k} are selector matrices that map the block stamps G_i^k and C_i^k to the rest of the network. The matrices R_k, L_k, C_k and G_k are the per-unit-length parameters of the k^{th} multiconductor transmission line (MTL); d_k is the length of the k^{th} MTL; U in the unity matrix; the variable $a_{0,k}$ is a predetermined constants given by the Padé approximation.

It should be noted that the MNA matrices described by (5) are obtained analytically in terms of per-unit-length parameters and predetermined constants given by the matrix-rational approximation. In the next section, the sensitivity analysis of interconnect parameters is derived using the above macromodel.

III. Sensitivity Analysis

Let λ_k be an interconnect parameter of the k^{th} interconnect. The sensitivity of the nonlinear network with respect to λ_k is obtained by differentiating (2) with respect to λ_k as

$$\frac{dC}{d\lambda_k}\frac{dx}{dt} + C\frac{d^2x}{d\lambda_k dt} + \frac{dG}{d\lambda_k}x + G\frac{dx}{d\lambda_k} + \frac{df}{dx}\frac{dx}{d\lambda_k} = 0 \tag{6}$$

Solution of (2) and (6) can be obtained by converting them to difference equations using integration formulae such as backward Euler or trapezoidal rule (TR) [8]. For example, if TR is used, the corresponding difference equations for (2) and (6) can be written as

$$\left(\frac{C}{\Delta t} + \frac{G}{2}\right)X_{n+1} + \frac{f(X_{n+1})}{2} = \left(\frac{C}{\Delta t} - \frac{G}{2}\right)X_n - \frac{f(X_n)}{2} + \frac{(b_{n+1} + b_n)}{2} \tag{7}$$

$$\left(\left(\frac{C}{\Delta t} + \frac{G}{2}\right) + \frac{\partial f(X_{n+1})}{2\partial X_{n+1}}\right)\frac{\partial X_{n+1}}{\partial \lambda_k} = -\frac{\partial}{\partial \lambda_k}\left(\frac{C}{\Delta t} + \frac{G}{2}\right)X_{n+1} + \left(\frac{C}{\Delta t} - \frac{G}{2}\right)\frac{\partial X_n}{\partial \lambda_k} + \frac{\partial}{\partial \lambda_k}\left(\frac{C}{\Delta t} - \frac{G}{2}\right)X_n - \frac{1}{2}\frac{\partial f(X_n)}{\partial X_n}\frac{\partial X_n}{\partial \lambda_k} \tag{8}$$

Equations (7) and (8) represent the solution of the original and sensitivity networks as described by (2) and (6). The coefficients on the right side of (8) are all known from the solution of (7). The variables $\partial f(X_{n+1})/\partial X_{n+1}$ and $\partial f(X_n)/\partial X_n$ are the Jacobean matrices which can be obtained by solving (7). The matrices $\partial C/\partial \lambda_k$ and $\partial G/\partial \lambda_k$ are derived from the stamp of the interconnect model as described below.

Calculation of $\partial C/\partial \lambda_k$ and $\partial G/\partial \lambda_k$

To calculate the sensitivity of the network, the derivatives of the MNA matrices are required with respect to the interconnect parameter λ_k of subnetwork k. Differentiating the MNA matrices of (3) with respect to λ_k,

$$\frac{\partial G}{\partial \lambda_k} = \sum_i (\psi_i^k)^T \frac{\partial G_i^k}{\partial \lambda_k} \psi_i^k$$
$$\frac{\partial C}{\partial \lambda_k} = \sum_i (\psi_i^k)^T \frac{\partial C_i^k}{\partial \lambda_k} \psi_i^k \tag{9}$$

The matrices $\partial C_i^k/\partial \lambda_k$ and $\partial G_i^k/\partial \lambda_k$ are computed analytically in terms of per-unit-length parameters and predetermined constants given by the matrix-rational approximation. As an example, Table I shows how these matrices are obtained for the real pole-zero subsection (5) for scalar interconnect parameters.

A similar strategy can be used for the complex pole-zero subsections (details are not given due to the lack of space).

TABLE I

Calculation of $\partial \boldsymbol{C}_{\boldsymbol{i}}^{\boldsymbol{k}} / \partial \lambda_k$ and $\partial \boldsymbol{G}_{\boldsymbol{i}}^{\boldsymbol{k}} / \partial \lambda_k$

$\partial \boldsymbol{G}_{\boldsymbol{i}}^{\boldsymbol{k}} / \partial \lambda_k$	$\partial \boldsymbol{C}_{\boldsymbol{i}}^{\boldsymbol{k}} / \partial \lambda_k$
$\frac{\partial \boldsymbol{G}_{\boldsymbol{0}}^{\boldsymbol{k}}}{\partial d_k} = \begin{bmatrix} \frac{G_k}{2a_{0,k}} & 0 & \frac{G_k}{2a_{0,k}} & 0 \\ 0 & \frac{-a_{0,k}}{2d_k^2 R_k} & \frac{a_{0,k}}{2d_k R_k} & 0 \\ \frac{G_k}{2a_{0,k}} & \frac{a_{0,k}}{2d_k^2 R_k} & \left(\frac{-a_{0,k}}{2d_k^2 R_k} + \frac{G_k}{2a_{0,k}}\right) & 0 \\ 0 & 0 & 0 & 0 \end{bmatrix}$	$\frac{\partial \boldsymbol{C}_{\boldsymbol{0}}^{\boldsymbol{k}}}{\partial d_k} = \begin{bmatrix} \frac{C_k}{2a_{0,k}} & 0 & \frac{C_k}{2a_{0,k}} & 0 \\ 0 & 0 & 0 & 0 \\ \frac{C_k}{2a_{0,k}} & 0 & \frac{C_k}{2a_{0,k}} & 0 \\ 0 & 0 & 0 & \frac{2L_k}{a_{0,k}} \end{bmatrix}$
$\frac{\partial \boldsymbol{G}_{\boldsymbol{0}}^{\boldsymbol{k}}}{\partial R_k} = \begin{bmatrix} 0 & 0 & 0 & 0 \\ 0 & \frac{-a_{0,k}}{2d_k R_k^2} & \frac{a_{0,k}}{2d_k R_k^2} & 0 \\ 0 & \frac{a_{0,k}}{2d_k R_k^2} & \frac{-a_{0,k}}{2d_k R_k^2} & 0 \\ 0 & 0 & 0 & 0 \end{bmatrix}$	$\frac{\partial \boldsymbol{C}_{\boldsymbol{0}}^{\boldsymbol{k}}}{\partial R_k} = \begin{bmatrix} 0 & 0 & 0 & 0 \\ 0 & 0 & 0 & 0 \\ 0 & 0 & 0 & 0 \\ 0 & 0 & 0 & 0 \end{bmatrix}$
$\frac{\partial \boldsymbol{G}_{\boldsymbol{0}}^{\boldsymbol{k}}}{\partial G_k} = \begin{bmatrix} \frac{d_k}{2a_{0,k}} & 0 & \frac{d_k}{2a_{0,k}} & 0 \\ 0 & 0 & 0 & 0 \\ \frac{d_k}{2a_{0,k}} & 0 & \frac{d_k}{2a_{0,k}} & 0 \\ 0 & 0 & 0 & 0 \end{bmatrix}$	$\frac{\partial \boldsymbol{C}_{\boldsymbol{0}}^{\boldsymbol{k}}}{\partial G_k} = \begin{bmatrix} 0 & 0 & 0 & 0 \\ 0 & 0 & 0 & 0 \\ 0 & 0 & 0 & 0 \\ 0 & 0 & 0 & 0 \end{bmatrix}$
$\frac{\partial \boldsymbol{G}_{\boldsymbol{0}}^{\boldsymbol{k}}}{\partial C_k} = \begin{bmatrix} 0 & 0 & 0 & 0 \\ 0 & 0 & 0 & 0 \\ 0 & 0 & 0 & 0 \\ 0 & 0 & 0 & 0 \end{bmatrix}$	$\frac{\partial \boldsymbol{C}_{\boldsymbol{0}}^{\boldsymbol{k}}}{\partial C_k} = \begin{bmatrix} \frac{d_k}{2a_{0,k}} & 0 & \frac{d_k}{2a_{0,k}} & 0 \\ 0 & 0 & 0 & 0 \\ \frac{d_k}{2a_{0,k}} & 0 & \frac{d_k}{2a_{0,k}} & 0 \\ 0 & 0 & 0 & 0 \end{bmatrix}$
$\frac{\partial \boldsymbol{G}_{\boldsymbol{0}}^{\boldsymbol{k}}}{\partial L_k} = \begin{bmatrix} 0 & 0 & 0 & 0 \\ 0 & 0 & 0 & 0 \\ 0 & 0 & 0 & 0 \\ 0 & 0 & 0 & 0 \end{bmatrix}$	$\frac{\partial \boldsymbol{C}_{\boldsymbol{0}}^{\boldsymbol{k}}}{\partial L_k} = \begin{bmatrix} 0 & 0 & 0 & 0 \\ 0 & 0 & 0 & 0 \\ 0 & 0 & 0 & 0 \\ 0 & 0 & 0 & \frac{2d_k}{a_{0,k}} \end{bmatrix}$

Sensitivity with respect to physical parameters

In the case when λ_k represents a physical parameter of the k^{th} interconnect, the sensitivity of the output nodes can be obtained as follows:

$$\frac{\partial \boldsymbol{x}}{\partial \lambda_k} = \sum_{i=1}^{m_k} \sum_{j=1}^{m_k} \left(\frac{\partial \boldsymbol{x}}{\partial R_k^{i,j}} \frac{\partial R_k^{i,j}}{\partial \lambda_k} + \frac{\partial \boldsymbol{x}}{\partial L_k^{i,j}} \frac{\partial L_k^{i,j}}{\partial \lambda_k} + \frac{\partial \boldsymbol{x}}{\partial G_k^{i,j}} \frac{\partial G_k^{i,j}}{\partial \lambda_k} + \frac{\partial \boldsymbol{x}}{\partial C_k^{i,j}} \frac{\partial C_k^{i,j}}{\partial \lambda_k} \right) \tag{10}$$

IV. Numerical Examples

A coupled interconnect system with a nonlinear diode is shown in Fig. 1. Fig. 2 shows transient responses of the far-end voltages corresponding to a 5 Volt input pulse with rise/fall times 0.1ns and a pulse width of 1ns. The sensitivities with respect to C_{11} for both the active and victim lines are shown in Fig. 3 and 4, respectively. The results of the proposed method are compared with the perturbation of the lumped segment model [2] (referred to as SPICE Perturbation). Fig. 5 and 6 show the sensitivities with respect to L_{11} for both the active and victim lines. Both the proposed method and the perturbation results are in good agreement.

It is to be noted that using the proposed method provides the following advantages. (1) Using the closed-form matrix-rational approximation based macromodel provides significant CPU advantages compared to lumped segmentation model [4]. (2) Perturbation based techniques can lead to inaccurate results (depending on the magnitude of the perturbation). (3) In addition, the nonlinear differential equations representing the perturbed network must be solved separately for every parameter of interest. However, in the proposed approach, the sensitivity information with respect to all the parameters can be essentially obtained from the solution of the original network. Table - II shows a comparison of savings in the main computational cost (in terms of total number of LU decompositions) using the proposed approach versus the perturbation approach, for the above example.

TABLE II

Computational Complexity: Proposed vs Perturbation

# of parameters	Perturbation (# LU decompositions)	Proposed (# LU decompositions)
10	26455	2405

V. Conclusions

A new approach for sensitivity analysis of lossy multiconductor transmission lines in the presence of nonlinear terminations is described. Sensitivity information is derived from the recently developed closed-form matrix-rational approximation based transmission-line model. The method enables sensitivity analysis of interconnect structures with respect to both electrical and physical parameters, while providing significant computational cost advantages.

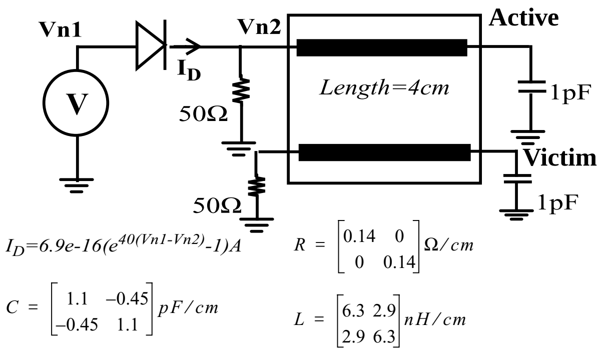

Fig. 1: Coupled interconnect system

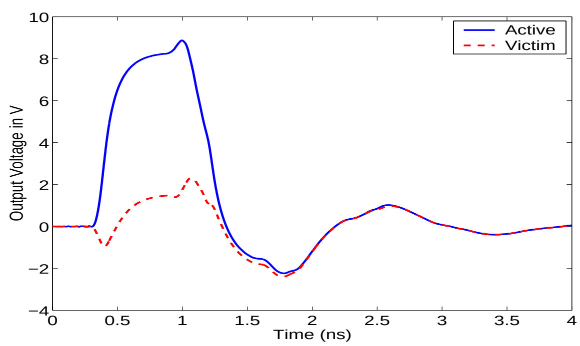

Fig. 2: Output transient response of circuit

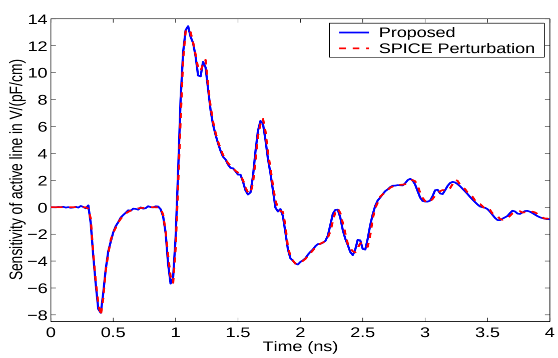

Fig. 3: Sensitivity of active line response w.r.t. C_{11}

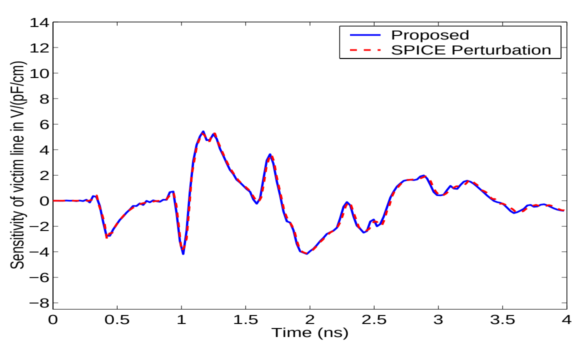

Fig. 4: Sensitivity of victim line response w.r.t. C_{11}

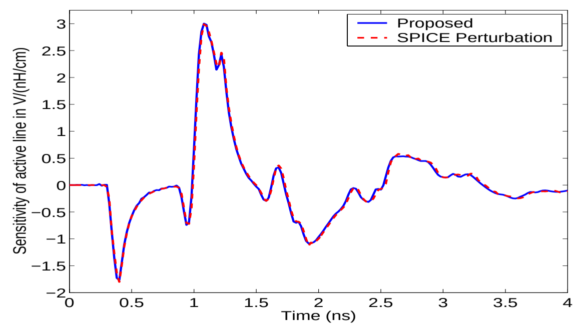

Fig. 5: Sensitivity of active line response w.r.t. L_{11}

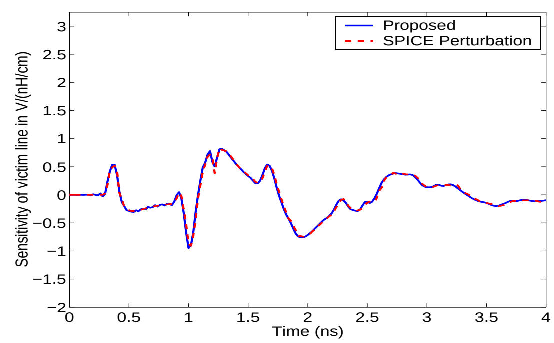

Fig. 6: Sensitivity of victim line response w.r.t. L_{11}

REFERENCES

[1] A. Deustsch, "Electrical characteristics of interconnections for high-performance systems," *Proc. of IEEE*, vol. 86, pp. 315-355, Feb. 1998.

[2] C. R. Paul, Analysis of Multiconductor Transmission Line. New York: Wiley, 1994.

[3] A. Dounavis, X. Li, M. Nakhla and R. Achar "Passive closed-loop transmission line model for general purpose circuit simulators," *IEEE Trans. on MTT*, vol. 47, pp. 2450-2459, Dec 1999.

[4] A. Dounavis, R. Achar and M. Nakhla "Efficient passive circuit models for distributed networks with frequency-dependent parameters," *IEEE Trans. on Advanced Packaging*, pp. 382-392, Aug. 2000.

[5] A. Dounavis, E. Gad, R. Achar and M. Nakhla, "Passive model reduction of multiport distributed interconnects," *IEEE Trans. on MTT*, vol. 48, pp. 2325-2334, Dec2000.

[6] A. Odabasioglu, M. Celik and L. T. Pilleggi, "PRIMA: Passive Reduced-Order Interconnect Macromodeling Algorithm, "*IEEE Trans. Computer-Aided Design*, vol. 17, No. 8, pp. 645-653, August 1998.

[7] C. Jiao, A. C. Cangellaris, A. Yaghmour, J. L. Prince, "Sensitivity Analysis of MTLs and optimization for high-speed Circuit Design", *IEEE Trans. on Advanced Packaging*, pp. 132-142, May. 2000.

[8] J. Vlach, K. Singhal, *Computer Methods for Circuit Analysis and Design*, NY, Van Nostrand Reinhold.